J Solid State Electrochem (2009) 13:807–812
DOI 10.1007/s10008-008-0771-4

ORIGINAL PAPER

Novel pore shape and self-organization effects in n-GaP(111)

K. Müller · J. Wloka · P. Schmuki

Received: 8 December 2008 / Accepted: 9 December 2008 / Published online: 6 January 2009
© Springer-Verlag 2008

Abstract n-type GaP(111) has been porosified in HCl, H_2SO_4, HBr, NaBr, and alkaline NaBr in the dark. The pore morphology strongly depends on the electrochemical conditions and on the chemical nature of anions in the electrolyte. Independent of the pH-value of bromide-containing solutions, layers of triangular pores with a defined cross-section were growing under an irregular pore nucleation layer. Optimized conditions led to a regular structure of equally sized triangular pores with a side length of (98 ± 5) nm. The pore walls are determined by (110)-crystal planes of GaP. In other electrolytes such as HCl or H_2SO_4 it was not possible to form triangular pores during the electrochemical etching process.

Keywords III-V semiconductors · Self-organization · Porosification · Pore morphology · Anodization · Crystal planes

Introduction

Since the discovery of light-emitting porous silicon [1], a lot of work in electrochemistry has been performed to porosify silicon and various other semiconductors such as GaAs [2], InP [3], and GaP [4, 5]. For n-GaP, Erné et al. [4] investigated the pore initiation and growth mechanism of (100)-oriented substrates in H_2SO_4 under potentiostatic and potentiodynamic conditions in detail. Pores can only grow at a potential anodic to a distinct breakdown potential; the so called "pore formation potential" (PFP) [2]. At this potential the band bending is high enough to cause tunneling of electrons from the conduction band to the electrolyte. In n-GaP(100) [4] primary pores start to grow perpendicular to the surface mainly at defect sites, because at defects such as dislocations the dissolution is energetically favored [6]. Then secondary pores branch radially to the primary ones forming a so-called "catacomb-like porous domain" below the surface. When the depletion layers of two porous domains overlap, vertical pore growth stops and domain boundaries, which are twice as thick as the depletion layer, separate the generated hemispherical pore domains. Other electrochemical etching of GaP is mostly done in H_2SO_4 [4, 5, 7], in ethanolic HF [8–10], or in diverse mineral acids [11].

Self-organization on n-type GaP(100) electrochemically etched in HBr was recently reported by Wloka et al. [12]. Rectangular pores with a certain aspect ratio and a very narrow size distribution were found. Other types of self-organization in n-GaP are shown by Föll et al. [13]. They reported current oscillation and corresponding pore-diameter oscillation.

The present paper deals with the porosification of n-GaP (111). n-GaP(111)-surfaces have been porosified in H_2SO_4 and HCl [14–16] to examine nonlinear optical behavior of the porous layers. Tiginyanu et al. [14] give a short description of the pore morphology of n-GaP(111) after electrochemical porosification in H_2SO_4 under illumination. They reported triangular prismatic pores with a lateral dimension of about 50 nm. The porous layers, reported to

K. Müller · J. Wloka · P. Schmuki (✉)
Department of Materials Science, LKO,
University of Erlangen-Nuremberg,
Martensstrasse 7,
91058 Erlangen, Germany
e-mail: schmuki@ww.uni-erlangen.de

Present address:
K. Müller
Laboratory for Micro- and Nanotechnology, Paul Scherrer Institut,
CH-5232 Villigen PSI, Switzerland

be transparent to visible light, were up to 10 µm thick and showed 30% porosity. In this paper we present a novel self-organization phenomena of n-GaP(111) in bromide containing electrolytes by etching in the dark.

Experimental

n-GaP(111)-samples, tellurium doped with a concentration of $3{\cdot}10^{17}$ cm^{-3} were used for electrochemical experiments. The samples were cut in rhomboids of approximately (6× 6) mm^2 along (110)-cleaving planes. Then they were degreased by successively sonicating in acetone, isopropanol, and methanol. Afterwards they were rinsed with pure water and dried in a nitrogen stream. Liquid In-Ga eutectic was smeared on the back side of the sample to establish an electrical back contact to a copper plate, which pressed the sample on an O-ring by means of a spring. All experiments were carried out in an O-ring cell with an area of 0.13 cm^2 open to the electrolyte. A three-electrode set-up was used with an Ag|AgCl reference electrode. All potentials are given with respect to this electrode. As counter electrode a platinum gauze was used. After the experiments the samples were again sonicated for 2 min in pure water to dissolve salt residues and dried with nitrogen. Cross-sections of the samples were taken after cleavage.

For the different electrolytes reagent grade chemicals and pure water were used. For polarization experiments a Jaissle high voltage potentiostat IMP88PC–200 V driven by a 1/16I Prodis function generator was used. The set-up was controlled by home-written software. All experiments were carried out at ambient temperature in the dark using a metal box, which also served as Faraday cage. Scanning electron microscope (SEM) images were taken with a Hitachi S4800 microscope. Fourier transforms were obtained by analyzing the SEM pictures with Scion Image 4.02 [17]. For this purpose, a circle was set in the centre of every pore to reduce the influence of the pore symmetry on the Fourier transformation.

Results and discussion

For comparison of different electrolytes polarization curves in 1 M HCl, 0.5 M H_2SO_4, and bromide-containing solutions with different pH-values were measured. Sulfuric acid was used as reference because a considerable amount of work on the porosification of GaP has been carried out in this electrolyte [4, 5, 7]. The curves are shown in Fig. 1. The breakdown potential in HCl is much smaller (around 8 V) than in the other solutions (15 V). In H_2SO_4 a partial current drop at about 15 V, just little anodic to the breakdown potential, is observed. In HCl such a transition is not as clearly visible as in sulfuric acid but also in HCl a broad constant current region above 12.5 V was measured.

In HBr no leveling of the current can be seen at potentials higher than 15 V; the current increases steeply until a diffusion-controlled current density limit is reached. These results are in accordance to experiments carried out with n-GaP(100) in the same electrolyte [12]. Only in the alkaline-bromide-containing solution a constant current region can be observed for the n-GaP(111). At potentials

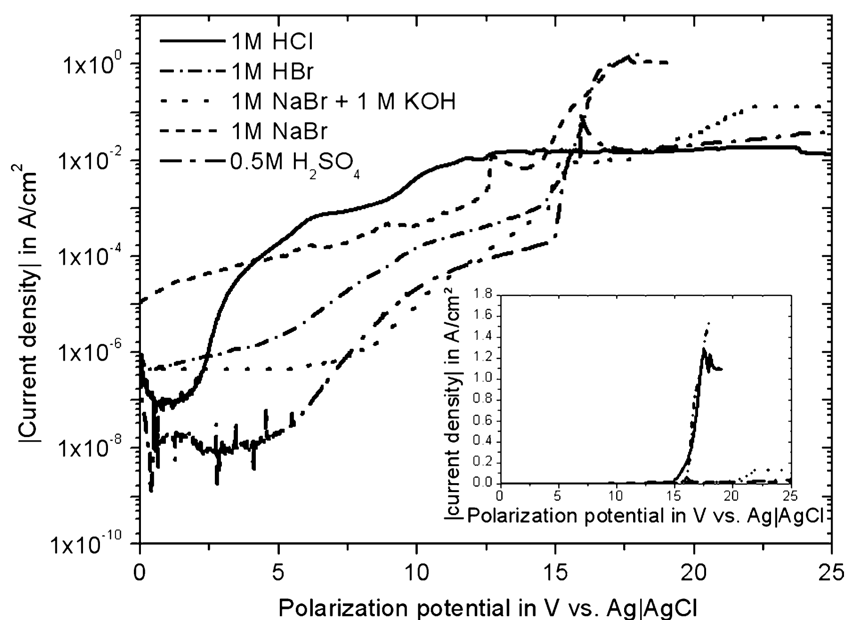

Fig. 1 Polarization curve of n-GaP(111) in 1 M HCl, 1 M HBr, 1 M NaBr, 1 M NaBr + 1 M KOH and 0.5 M H_2SO_4, scan rate: 20 mV/s

anodic to the PFP the highest current densities were found in HBr and NaBr containing solutions, which also means that here the highest dissolution rate was established. This can also be seen in the SEM images (Fig. 2); the largest degree of surface attack took place in these electrolytes.

Samples polarized in HBr typically show a large number of triangular pores with variable size (Fig. 2a). The side walls of the pores are parallel to the <111>-directions. The triangular symmetry indicates that the side walls are the (110)-crystal planes, which are the most stable planes in zinc blende structure [18]. A short explanation for this etch stop at (110)-planes is provided in Fig. 3. By considering the ionic character of GaP two different surface types can be observed. In one type only atoms of one species are in the outermost surface layer. In this case a dipole moment perpendicular to the surface is setup making these surfaces energetically less favorable and thus less stable [18]. Thus, these planes are expected to be highly reactive unless they show reconstruction; they are only stable in GaP due to the considerable amount of covalent binding in this material. For pure ionic crystals like ZnS, these planes contain only one ionic species and are not stable. In n-GaP the (100)- and (111)-surfaces consist of only one species, either Ga or P (cf. Fig. 3a, b). In contrast, the (110)-surfaces are occupied by both types of atoms (filled and unfilled circles in Fig. 3). Therefore, these surfaces show no dipole moment perpendicular to the surface and thus, are more stable than the other two surface orientations even without or with only little surface reconstruction. These results are in line with other III-V-semiconductors which crystallize in the zinc blende structure.

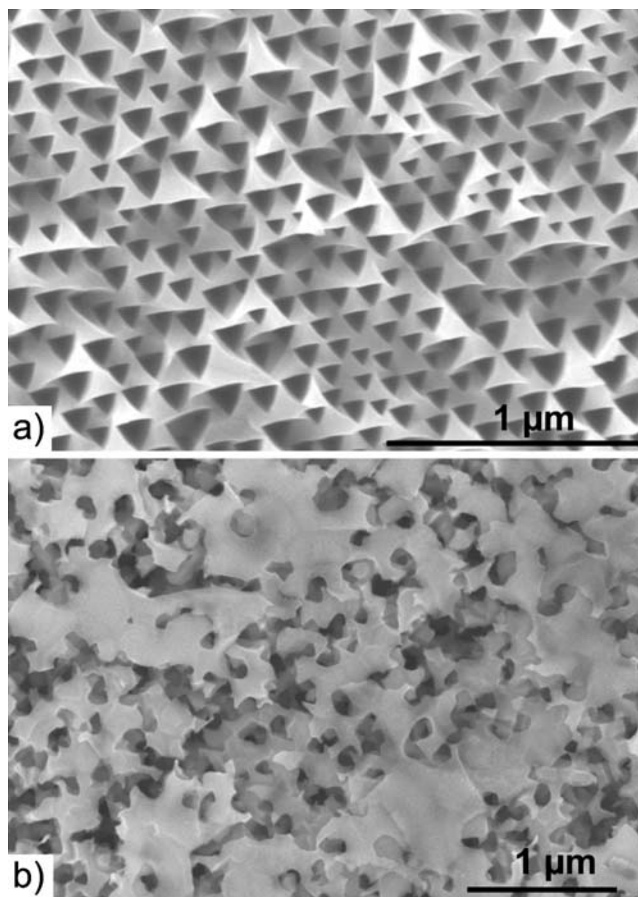

Fig. 2 n-GaP(111) **a** after polarization in 1 M HBr (0 to 20 V, 20 mV/s), the same pore morphology has been observed in neutral and alkaline bromide containing solution after polarization, **b** after potentiostatic etching in 0.5 M H_2SO_4 at 15 V for 900 s

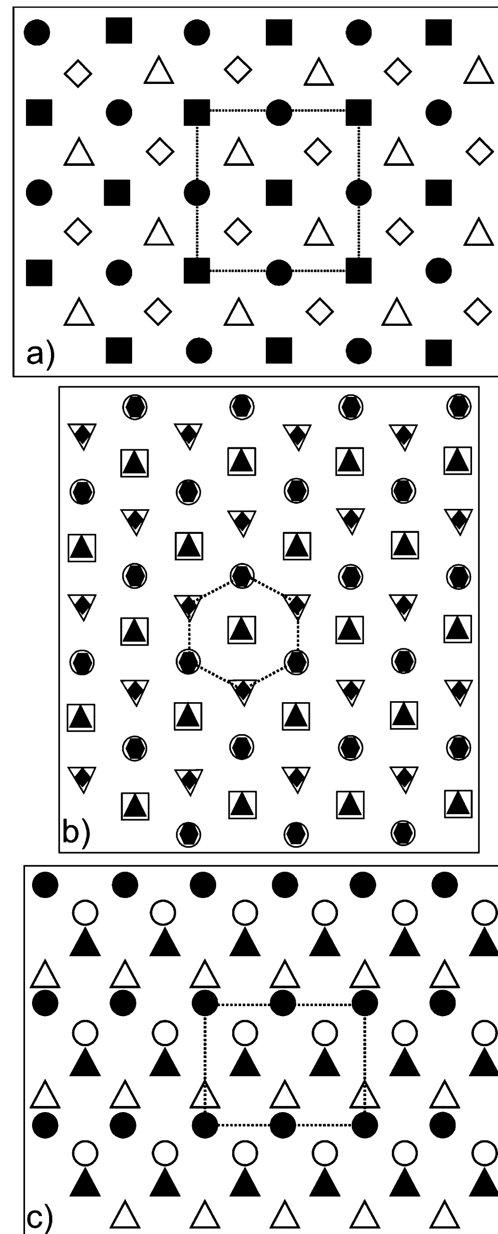

Fig. 3 Model for different layers in zinc blende structure, *dotted lines* indicate unit cell, *circle* first layer, *triangle* second layer, *square* third layer, *diamond* fourth layer, *inverted triangle* fifth layer, *hexagon* sixth layer, *filled* Ga, *unfilled* P; **a** (100)-surface, **b** (111)-surface, **c** (110)-surface

Another pore-morphology was found in 0.5 M H_2SO_4. After polarization no pores could be seen in the SEM image, but a wavy surface. Assuming that this structure is due to oxide formation and subsequent lift-off (cf. Fig. 1 "passivity" peak in H_2SO_4), n-GaP(111) was etched potentiostatically at 15 V in 0.5 M H_2SO_4, i.e. at a potential slightly below the oxide formation potential. The SEM image of the sample porosified via this etching procedure is shown in Fig. 2b. Randomly distributed pores, which look like pitting of the surface were found. We assume that these structures are also defect controlled. The pores produced in H_2SO_4 in the dark are different to these shown by Tiginyanu et al. [14] for the porosification of n-GaP(111) in sulfuric acid under illumination. To examine these results n-GaP (111) was also polarized in H_2SO_4 under light. On these samples irregular triangular pores were found (not shown here). The spacing between the different pores is less than in the dark due to a smaller depletion layer width. Porosified n-GaP(111) in HBr under light also shows a triangular structure but with less regular pores than in the dark.

A possible reason for the different pore morphologies may be the unequal reactivity of the different anionic species in the electrolytes. Halides are more reactive than sulfates; this can also be seen in the polarization curves. Cathodic to the breakdown potentials the current density in H_2SO_4 is at least one order of magnitude smaller than in the other electrolytes. To achieve crystallographically oriented etching structures, which means triangular pores in (111)-oriented material, the electrochemical etching in sulfate must be assisted by the photocurrent produced via illumination, whereas the reactivity of bromide ions is high enough to produce triangular structures without illumination.

Bromide ions seem to have a great influence to the dissolution of GaP, because this is the only solution were no "current limiting" region can be found at neutral or acidic pH-values. Only for NaBr + KOH a passive region between 15 V and 20 V has been observed. Either the oxide dissolves much faster in these bromide-containing solutions or specific ion adsorption on the surface inhibits the oxide formation. At potentials cathodic to the pore formation potential, pores which are produced in bromide solutions are similar to those in HCl.

The occurrence of equilateral triangular pores is not only restricted to acidic bromide solutions. Moreover the best results were found in alkaline solutions (Fig. 4b). This can be seen by the inset, which shows the Fourier-transform of the SEM picture. One lighter diffraction circle in the middle surrounded by several black circles can be seen. This shows that the pore morphology has a high degree of short-range order whereas there is no definite indication for long-range order in the diffraction pattern. It is noteworthy that also in neutral bromide containing electrolytes triangular pores were found, but with a rougher surface.

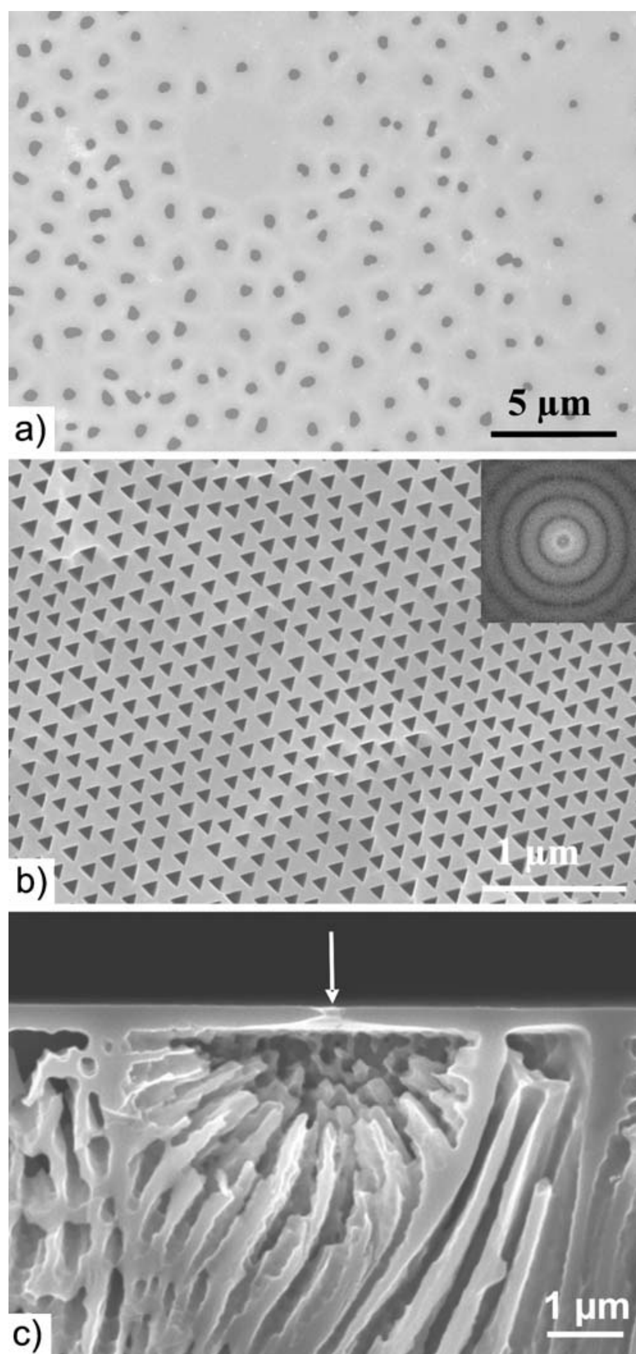

Fig. 4 Nucleation layer (**a**) and self-ordered crystallographically oriented pores, with a side length of 98±5 nm (**b**) in GaP(111) polarized in 1 M NaBr + 1 M KOH 0 to 21 V, 20 mV/s and cross-section of n-GaP potentiostatically etched in 1 M NaBr + 1 M KOH at 15 V for 900 s (**c**)

For all bromide containing electrolytes another interesting feature can be observed. On top of the electrochemically etched samples an initiation layer was originally formed (Fig. 4a), with just little attack, this means only some randomly distributed holes were found. This is in agreement with the findings of Erné et al. [4] on n-GaP

(100) in 0.5 M H_2SO_4. The faint white lines around the initial pores show the domain walls, where the depletion layers of the neighboring porous domains overlap. At some parts of the sample this layer was lifted off and a highly ordered structure underneath could be found (Fig. 4b). The size of the triangles is almost constant with a side length of (98 ± 5) nm which was measured by evaluation of 100 pores.

In a cross-section of a potentiostatically etched sample this initiation layer can also be seen (Fig. 4c). The primary pore is marked with a white arrow. Below this the hemispherical domain can be seen. Afterwards crystallographic oriented pores start to grow perpendicular into the material. These pores exhibit a triangular shape. The primary pores in the initiation layer are assumed to be defect oriented, because at the beginning of the electrochemical etching process the defect sites are attacked.

Best ordered structures were obtained by cathodic polarization from 20 V down to 10 V (with a polarization rate of 50 mV/s) in 1 M HBr (cf. Fig. 5). The potentials and the current-densities are high enough to favor self-organized pore growth. The fairly good self-organization can be verified by the Fourier-transform of the point pattern, shown in the inset. In this case the circles are more discrete compared to inset in Fig. 4b, this may be a first indication for a long-range order. No initiation layer was found under these conditions, because the pore initiation at high potentials starts randomly and not defect controlled as it does at lower potentials.

In the cross-sections of the triangular pores straight pores with regular distribution can be seen (cf. Fig. 6). The porous layer produced by polarization shows just a thickness of about 2 µm (cf. Fig. 6a). These pores are very straight and have the same length within a tolerance of 10%. The triangular pore grounds are another indication for the tetrahedral growth of the pores. It is also possible to grow layers of more than 100 µm thickness by potentiostatic etching slightly above the PFP (cf. Fig. 6b, only a section of the whole layer is shown here). The growth velocity of the pores in this case has been at least 10 µm/s, provided that no surface abrasion took place. It is possible to get very parallel pores without any pore-diameter oscillation by potentiostatic etching. Also the thickness of the pores does not vary with etching time or thickness of the porous layer. These structures may be very interesting as templates for nanowires because of the very regular pore walls which show no oscillation. For these templates no pre-patterning is needed.

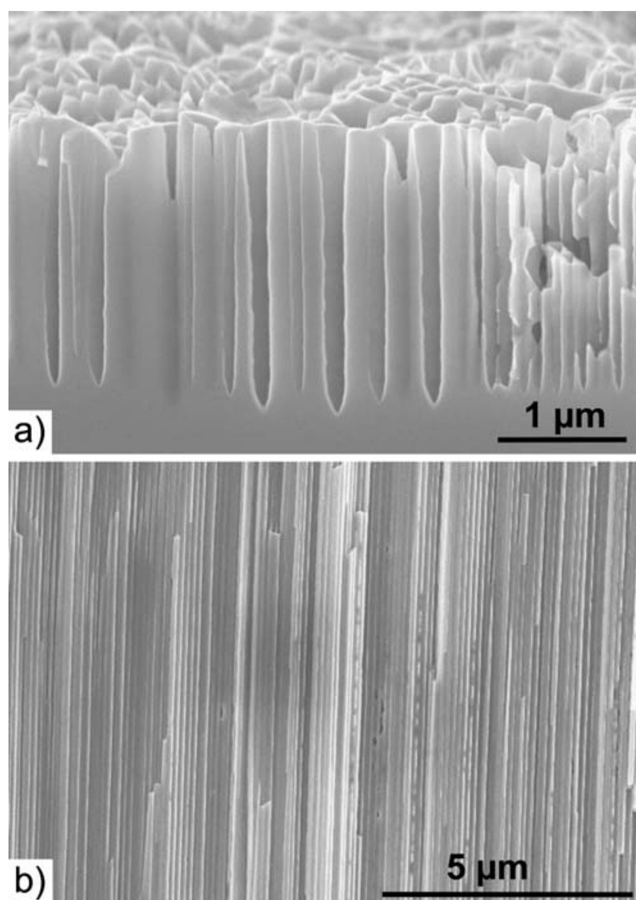

Fig. 6 : Cross-section of n-GaP(111) etched in **a** 1 M NaBr + 1M KOH, polarization from 0 to 21 V, 20 mV/s and **b** 1 M HBr potentiostatic at 15 V for 900 s

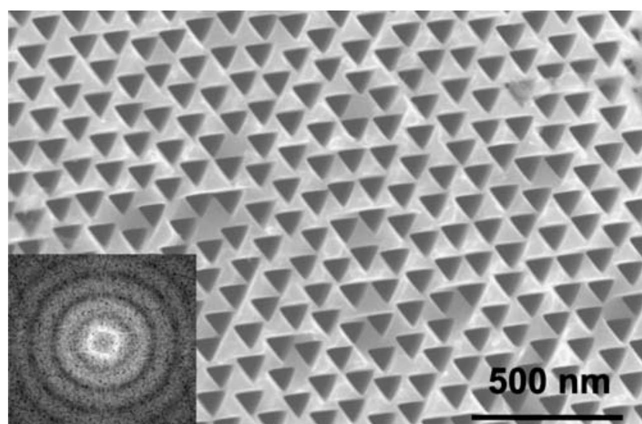

Fig. 5 : n-GaP (111) polarized in 1 M HBr from 20 to 10 V with 50 mV/s; subsequent potentiostatic etching at 10 V for 900 s

Conclusion

The porosification behavior of n-GaP(111) in different electrolytes was investigated. A quite regular structure of triangular pores, with a narrow size distribution of (98 ± 5) nm can be found in n-GaP(111)-surfaces by electrochemical etching in bromide-containing solutions. Short-

range self-organization of these pores could be shown by Fourier-transformation. The best ordered structures were found by dynamic cathodic polarization from potentials above the PFP to potentials below the PFP followed by potentiostatic etching in 1 M HBr. The cross-sections show pores with regular arrangement growing parallel for 100 μm without any diameter oscillations. The pore walls are determined by (110)-planes. The above-described pore symmetry was only found in bromide containing electrolytes independent of the pH-value. No active/passive transition takes place by polarization in neutral or acidic bromide-containing electrolytes whereas in alkaline NaBr, HCl, and H_2SO_4 a broad region of a limited current density is found in polarization curves. The pores in HCl and H_2SO_4 electrolytes seem to be defect oriented, whereas the pores in bromide-containing solutions are crystallographically oriented.

Acknowledgements This work was carried out at University Erlangen-Nuremberg (Germany). M. Czupalla from the Institute for Crystal Growth (IKZ) in Berlin is greatly acknowledged for providing the n-GaP(111)-samples. B. Rackl is acknowledged for fruitful discussion.

References

1. Cullis AG, Canham LT, Calcott PDJ (1997) J Appl Phys 82:909. doi:10.1063/1.366536
2. Schmuki P, Fraser J, Vitus CM, Graham MJ, Isaacs HS (1996) J Electrochem Soc 143:3316. doi:10.1149/1.1837204
3. Schmuki P, Santinacci L, Djenizian T, Lockwood DJ (2000) Phys Status Solidi A 182:51 doi:10.1002/1521-396X(200011)182:1<51::AID-PSSA51>3.0.CO;2-S
4. Erné BH, Vanmaekelbergh D, Kelly JJ (1996) J Electrochem Soc 143:305. doi:10.1149/1.1836428
5. Erné BH, Vanmaekelbergh D, Kelly JJ (1995) Adv Mater 7:739. doi:10.1002/adma.19950070813
6. Hueppe M, Schlierf U, Gassiloud R, Michler J, Schmuki P (2005) Phys Status Solidi C 2:3359. doi:10.1002/pssc.200461167
7. Tjerkstra RW, Gómez Rivas J, Vanmaekelbergh D, Kelly JJ (2002) Electrochem Solid-State Lett 5:G32. doi:10.1149/1.1466935
8. Meijerink A, Bol AA, Kelly JJ (1996) Appl Phys Lett 69:2801. doi:10.1063/1.116848
9. Anedda A, Serpi A, Karavanskiĭ VA, Tiginyanu IM, Ichizli VM (1995) Appl Phys Lett 67:3316. doi:10.1063/1.115232
10. Tiginyanu IM, Ursaki VV, Karavanskiĭ VA, Sokolov VN, Raptis YS, Anastassakis E (1996) Solid State Commun 97:675. doi:10.1016/0038-1098(95)00677-X
11. Wloka J, Schmuki P (2006) J Electroceram 16:23. doi:10.1007/s10832-006-4825-7
12. Wloka J, Mueller K, Schmuki P (2005) Electrochem Solid-State Lett 8:B72. doi:10.1149/1.2103507
13. Föll H, Carstensen J, Langa S, Christophersen M, Tiginyanu IM (2003) Phys Status Solidi A 197:61. doi:10.1002/pssa.200306469
14. Tiginyanu IM, Kravetsky IV, Monecke J, Cordts W, Marowsky G, Hartnagel HL (2000) Appl Phys Lett 77:2415. doi:10.1063/1.1316770
15. Sarua A, Gärtner G, Irmer G, Monecke J, Tiginyanu IM, Hartnagel HL (2000) Phys Status Solidi A 182:207 doi:10.1002/1521-396X(200011)182:1<207::AID-PSSA207>3.0.CO;2-3
16. Tiginyanu IM, Kravetsky IV, Langa S, Marowsky G, Monecke J, Föll H (2003) Phys Status Solidi A 197:549. doi:10.1002/pssa.200306567
17. www.scioncorp.com/. Accessed 2 Dec 2008
18. Tasker PW (1979) J Phys C 12:4977 doi:10.1008/0022-3719/12/22/036